Hydrogen movement in cubic Mg_2NiH_4

G. N. García,* J. P. Abriata, and J. O. Sofo
Centro Atómico Bariloche and Instituto Balseiro, Comisión Nacional de Energía Atómica, (8400) Bariloche RN, Argentina
(Received 30 May 2001; revised manuscript received 12 October 2001; published 16 January 2002)

The motion of hydrogen atoms in Mg_2NiH_4 is studied based on *ab initio* total-energy calculations using the full potential linearized augmented plane-wave method. We calculate the jump frequency for two kind of rotations of the NiH_4 complex through classical rate theory. The obtained jump frequencies are $4\times10^{13}e^{-1.29eV/kT}$ s^{-1} and $3\times10^{13}e^{-0.67eV/kT}$ s^{-1} for in-plane and out-of-plane rotations, respectively. These values agree well with experimental data as concluded from solving the equation for the linewidth within the Bloembergen-Purcell-Pound theory of nuclear magnetic resonance.

DOI: 10.1103/PhysRevB.65.064306 PACS number(s): 66.30.Ny

I. INTRODUCTION

Many intermetallic compounds have been found to be excellent hydrogen absorbing materials. This property makes hydrides attractive candidates for different applications and extensive studies are being made in order to use the hydrides in devices that range from hydrogen-storage containers to heat pumps and high-performance secondary batteries.[1]

One of the promising ternary hydrides is Mg_2NiH_4,[2] which still presents several basic uncertainties with respect to the location of hydrogen in the lattice.[4] The binary compound Mg_2Ni (Ref. 3) reacts readily with gaseous hydrogen to form the solid solution $Mg_2NiH_{0.3}$ and, upon further hydrogen absorption, a hydride Mg_2NiH_4 may be formed. This hydride is monoclinic at temperatures below 510 K and cubic at higher temperatures.[5] For the cubic phase of Mg_2NiH_4, hydrogen atomic positions and temperature factors have been investigated experimentally using neutron diffraction techniques.[6–10] The hydrogen motion, for the same phase, has been studied using different ^1H nuclear magnetic resonance techniques[11–13] and neutron diffraction.[9] The electronic structure and cohesive properties of this phase have been studied theoretically.[4,14]

In hydrides based on transition metals there is evidence for a strong and localized hydrogen-metal bond. These compounds can be seen as composed of hydrogen-metal complexes in a non-transition-metal framework. An example of these hydrides is Mg_2NiH_4. In a previous work,[4] we have studied the configuration of the NiH_4 complex in Mg_2NiH_4 based on total-energy calculations. Our results on the energetics of the cubic hydride indicate that the minimum energy configuration corresponds to a tetrahedrically distorted square distribution of hydrogen atoms around the nickel atom, which is in agreement with neutron diffraction data. The nickel-hydrogen distance obtained is in excellent agreement with the experimental value and seems to be characteristic of the NiH_4 complex.

The positions occupied by the hydrogen atoms in the metal lattice influence the static, dynamic, electronic, and magnetic properties of metal-hydrogen systems. Moreover, the diffusion of hydrogen atoms is very important for dynamic processes like hydrogen absorption or desorption and this information is relevant to understand and control the process for technical applications.

The activation energy and jump frequency are used to characterize the diffusion process. The hydrogen dynamics in Mg_2NiH_4 was investigated experimentally using ^1H NMR (Refs. 11–13) and neutron scattering.[9] Two scenarios emerge to describe the observations: the NiH_4 complex can be moving as a rigid molecule or hydrogen is moving as an independent atom between the free octahedral sites around nickel. In any of these cases, there is agreement to describe the movement as highly localized around nickel.

Our previous results[4] show that hydrogen is covalently bonded with nickel forming a NiH_4 complex bonded ionically to magnesium. The observation of a well-defined NiH_4 unit induces us to think about a localized and correlated motion of hydrogen around nickel in the form of a rigid molecule. In this work, we focus on testing these ideas by studying the kinetic properties of hydrogen in this hydride.

We analyze the diffusion of hydrogen by considering the motion of a planar NiH_4 unit. Through a combination of movements a hydrogen atom can visit each of the six sites of the octahedron centered in a nickel atom. Two different rotations are considered: one around an axis perpendicular to the plane and the other around a diagonal of the square. In the former all four hydrogen atoms are moved, while in the latter only two of them are moved. In both cases the deformations of the planar NiH_4 unit are considered by independent optimization of the nickel-hydrogen distance. The activation energy and the attempt jump frequency are determined by means of *ab initio* total-energy calculations.

This work is organized as follows. In Sec. II we describe the experimental information found in literature about the hydrogen motion in Mg_2NiH_4. In Sec. III the models considered for hydrogen motion in the hydride, the total-energy calculation method, a brief description of classical rate theory, and the results are presented. In Sec. IV we give basic concepts of nuclear magnetic resonance theory and present the results obtained for a simplified model for the width of the resonance line. The conclusions are given in Sec. V.

II. EXPERIMENTAL INFORMATION

Among the different experimental methods used to study diffusion of hydrogen in hydrides, nuclear magnetic resonance and neutron diffraction have been used to determine

the hydrogen jump frequency and activation energy in Mg_2NiH_4.[9,11–13,15]

In NMR, the nuclear relaxation time of the protons and the width of the resonance line are measured as a function of temperature. These quantities are determined by the magnetic dipole interaction between the magnetic moments of hydrogen atoms.

In neutron diffraction, a monoenergetic neutron beam passes through a crystal and emerges with a certain distribution of energy. The measure of the energy spectra of the neutrons gives information of hydrogen motion and location.

Early NMR studies of the dynamical properties of hydrogen atoms in Mg_2NiH_4 were made by Goren *et al.*,[11] where the spin-lattice relaxation time was measured in a wide temperature range. They were interested in the low-temperature phase of the hydride. In the cubic phase at high temperature these authors estimated an activation energy of 0.52 eV.

Neutron scattering experiments, by Noréus and Olsson,[9] indicated that the hydrogen atom motion is highly localized around each nickel atom and correlated to the jumps of the neighbors. The detailed motion cannot be found because of instrumental limitations. However, they concluded that the hydrogen motion is likely to be restricted to the six octahedral sites around each nickel in such a way that four hydrogen atoms form a square planar unit which randomly flips around the nickel atom. With this reorientational motion model, they determined the correlation frequency and activation energy of 10^{11} s^{-1} and 0.16 eV, respectively.

Hayashi *et al.* studied the low-temperature phase[12] and the monoclinic-cubic phase transition[13] of Mg_2NiH_4 by pulsed NMR. They measured linewidth and relaxation times and found that the motion is highly localized around the nickel atom in agreement with observations made by Noréus and Olsson. Their results suggest that the hydrogen motion is a reorientational processes with a single activation energy of 0.52 eV. They proposed a model in which a square planar unit of NiH_4 rotates mainly around the axis perpendicular to the plane. In the temperature range across the transition, they observed that the planar unit NiH_4 changes slightly to an isotropic motion favored by thermal expansion.

So far, all our discussion of hydrogen motion has been concerned with localized motion around one Ni. The translational diffusion of hydrogen atoms between complexes is found to be slower by three to five orders of magnitude than the rotational diffusion. This was suggested both by neutron scattering and NMR experiments.[9,13]

The mentioned results give values of the jump frequency and activation energy for the hydrogen motion. To elucidate the microscopic origin of these values, we compare in this work the theoretical results obtained for different motional models with the experimental results.

III. TOTAL ENERGIES FOR HYDROGEN MOTION

A. Method for the total-energy calculation

For our *ab initio* calculations of total energies we use the full-potential linearized augmented plane-wave method (FP-LAPW).[16] In brief, this is an implementation of density functional theory with different possible approximations for the exchange and correlation potential, including the local spin-density approximation (LSDA). The Kohn-Sham equations are solved using a basis of linearized augmented plane waves.[17] For the exchange and correlation potential we use the Perdew-Wang[18] parametrization of the Ceperley-Alder data. Local orbital extensions to the LAPW basis[19] are used to describe the $3s$ and $3p$ orbitals of Mg and the $3p$ orbitals of Ni. The wave functions are expanded up to $l=10$ within the muffin-tin spheres, and the potential and charge density are expanded up to $l=6$. We use a converged basis set of around 2000 plane waves and a sampling of the Brillouin zone (BZ) of 400 points, which in the irreducible wedge of the BZ correspond to 40 points for the case of rotation around the z axis and 100 points for rotation around the y axis. Muffin-tin radii of 1.8 bohr for Mg and Ni and 0.8 bohr for H are used.

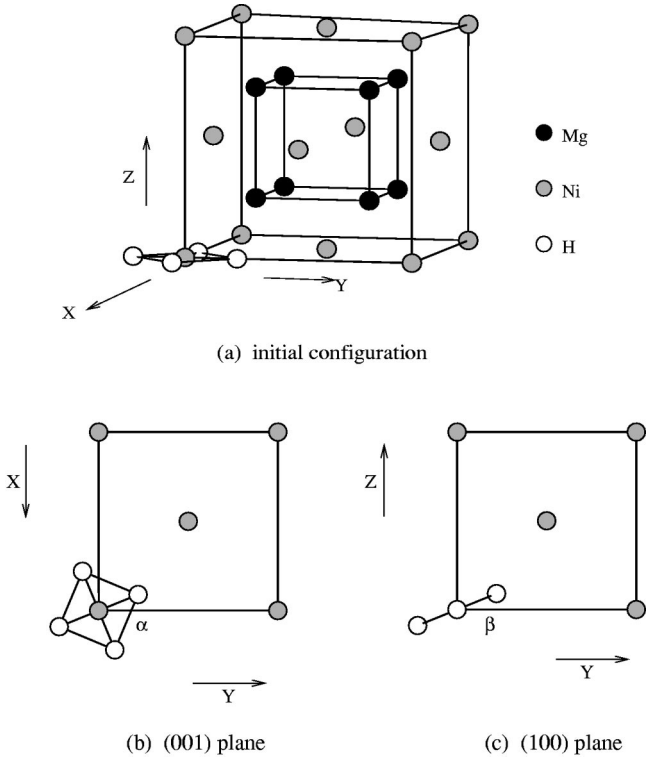

FIG. 1. (a) The antifluorite structure of Mg_2NiH_4. (b) and (c) Proposed models for the movement of the NiH_4 unit. The arrangement of four hydrogen atoms is around all Ni atoms in the unit cell. This arrangement is not shown for simplicity, except for one of them. Solid lines connecting hydrogen atoms do not intend to represent H-H bonds, but are shown as a guide.

B. Proposed diffusion models

The high-temperature phase of Mg_2NiH_4 has a cubic cell corresponding to the antifluorite structure, Fig. 1(a), with a lattice constant value of $a=6.507$ Å.[2,9]

In a previous paper,[4] we studied the energetics of the cubic hydride for different hydrogen arrangements. We found that the hydrogen and nickel atoms form a NiH_4 complex. This unit has a tetrahedrically deformed configuration with a bending angle of 21.8°. In this work, we consider a plane

TABLE I. Calculated and experimental values for the attempt jump frequencies and the activation energies.

	$\nu_0[s^{-1}]$	ΔE [eV/formula]
In-plane rotation	4×10^{13}	1.29
Out-of-plane rotation	3×10^{13}	0.67
Neutrons	$\sim10^{11}$	0.16
NMR (HT phase)	$\sim10^{13}$	0.85
NMR (LT phase)	2.3×10^{13}	0.52

configuration for the NiH_4 complex to avoid the computational effort involved in the calculation of structures without inversion symmetry. We do not expect differences because the activation energy of the motion is at least twice the energy jump between the used and minimum configurations.

We consider rotations of the planar arrangement of hydrogen atoms around the principal cell axis as diffusion paths and study the in-plane rotation and out-of-plane rotation. Figure 1 shows the principal cell axis and the rotated planar arrangements. The rotations around the X and Y axes are equivalent due to the symmetry of the unit cell. We do not consider simultaneous combinations of these two motions.

The rotation angle varies between 0 and 45° due to the symmetry of the metallic framework. Setting up a rotation angle, we make variations of the hydrogen-nickel distances, d and d', to obtain the minimum in the energy curve.

For in-plane α rotation, the considered hydrogen positions are $(x,y,0)$, $(-y,x,0)$, $(-x,-y,0)$, and $(y,-x,0)$, where $x=d/a\cos\alpha$ and $y=d/a\sin\alpha$. As is indicated in Fig. 1(b), α is the angle between the Y axis of the unit cell and the nickel-hydrogen line.

In the out-of-plane β rotation, the hydrogen atoms are located at $(0,y,z)$, $(x',0,0)$, $(0,-y,-z)$, and $(-x',0,0)$, where $y=d/a\cos\beta$, $z=d/a\sin\beta$, and $x'=d'/a$. The angle formed by the Y axis of the unit cell and the line that connects the nickel atom with one of the movable hydrogen atoms is β, as is shown in Fig. 1(c).

C. Classical rate theory

In Sec. II, we described the available experimental information on hydrogen diffusion in Mg_2NiH_4. The experiments indicate that the hydrogen has a very fast and local motion around the nickel atom; see Table I. This result suggests the model of a square planar NiH_4 unit that randomly flips so that isotropic symmetry is obtained.

Using density functional calculations, we have obtained the total energy of the system for different positions of the hydrogen atoms along a diffusion path. In this way, it is possible to calculate the jump frequency and the energy barrier for the hydrogen passage from one site to another following a proposed diffusion path.[20]

The overbarrier jumps of hydrogen from an equilibrium site will be studied considering the classical rate theory[21,22] that defines the jump frequency as the probability to reach the top of the barrier with a speed in the forward direction,

TABLE II. Optimized values for the fractional coordinates x and y and the minimized Ni-H distance for different angles of rotation, α, around the Z axis of the unit cell.

α	x	y	$d_{Ni\text{-}H}$ [Å]
0	0.2379	0	1.548
11	0.2337	0.0454	1.550
22.5	0.2177	0.0902	1.533
34	0.1907	0.1286	1.497
45	0.1600	0.1600	1.473

and using the usual probability definition and the harmonic approximation for the system's energy, the jump frequency can be written as

$$\nu=\left\{\frac{\prod_{j=1}^{N}\omega_j}{\prod_{i=2}^{N}\omega_i'}\right\}\exp^{-\Delta E/kT}. \tag{1}$$

The products in Eq. (1) run over vibration modes in both situations. ΔE represents the difference of potential energy with the jumping hydrogen atoms in positions of maximum potential energy with respect to the system with the atoms in equilibrium.

A crude approximation consists in considering that the vibration mode frequencies in the two configurations are equal, except for the mode corresponding to the diffusion direction. In such a way, the jump frequency ν is proportional to the hydrogen vibrational frequency along the diffusion path in the equilibrium configuration ω_1, which is called the attempt jump frequency ν_0:

$$\nu=\nu_0 e^{-\Delta E/kT}. \tag{2}$$

D. Theoretical results for interatomic distances and jump frequencies

The optimized values for fractional coordinates and nickel-hydrogen distances, for each rotated configuration, are summarized in Tables II and III. The nickel-hydrogen distance takes values between 1.45 Å, and 1.55 Å, while the experimental value is 1.55 Å.[9] The nickel-hydrogen distance seems to be almost independent of the rotation axis. Its

TABLE III. Optimized values for the internal parameters y, z, x', and the minimized Ni-H distances for different angles of rotation, β, around the X axis of the unit cell. The Ni-H distance along the rotation axis is represented by $d'_{Ni\text{-}H}$.

β	y	z	$d_{Ni\text{-}H}$ [Å]	x'	$d'_{Ni\text{-}H}$ [Å]
0	0.2379	0	1.548	0.2379	1.548
11	0.2259	0.0439	1.497	0.2379	1.548
22.5	0.2070	0.0857	1.458	0.2378	1.548
34	0.1852	0.1249	1.454	0.2378	1.548
45	0.1601	0.1601	1.474	0.2377	1.547

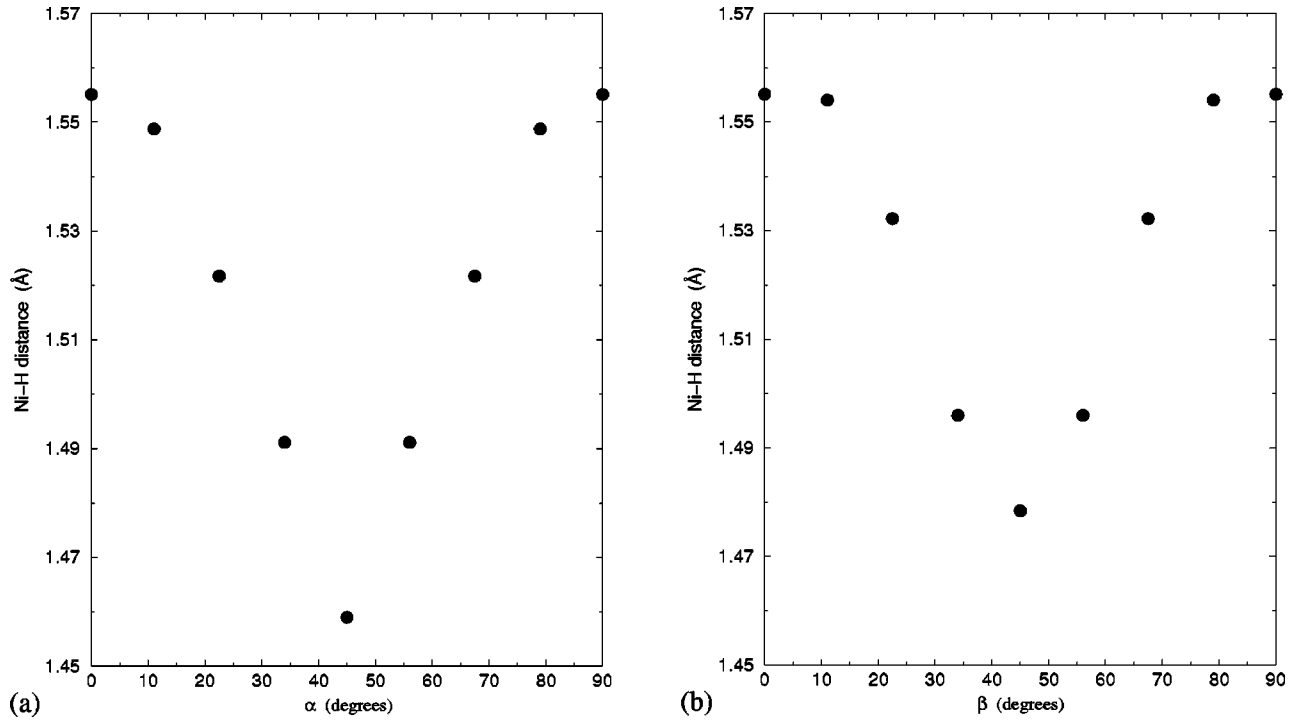

FIG. 2. Variation of Ni-H distance along the representative range of both rotation paths, the in-plane α rotation (a) and the out-of-plane β rotation (b).

value decreases for increasing values of the rotation angle between 0 and 45°, as can be seen in Fig. 2. The initial square planar configuration of the NiH_4 complex suffers deformations along the diffusion path. In the out-of-plane β rotation, the values of the two different nickel-hydrogen distances, normal and along the rotation axis, imply a rhombohedrical deformation, while the in-plane α rotation involves a compression of the NiH_4 unit. The size and shape of the NiH_4 complex change along the rotation paths to minimize the internal and external hydrogen-hydrogen interactions.

The existence of covalent bondings between nickel and hydrogen atoms and mainly ionic bonding between magnesium and the NiH_4 complex is a common feature in the different configurations along the diffusion paths, as shown in Fig. 3. With the rotation, the distances between hydrogen atoms belonging to different complexes are shorter and the

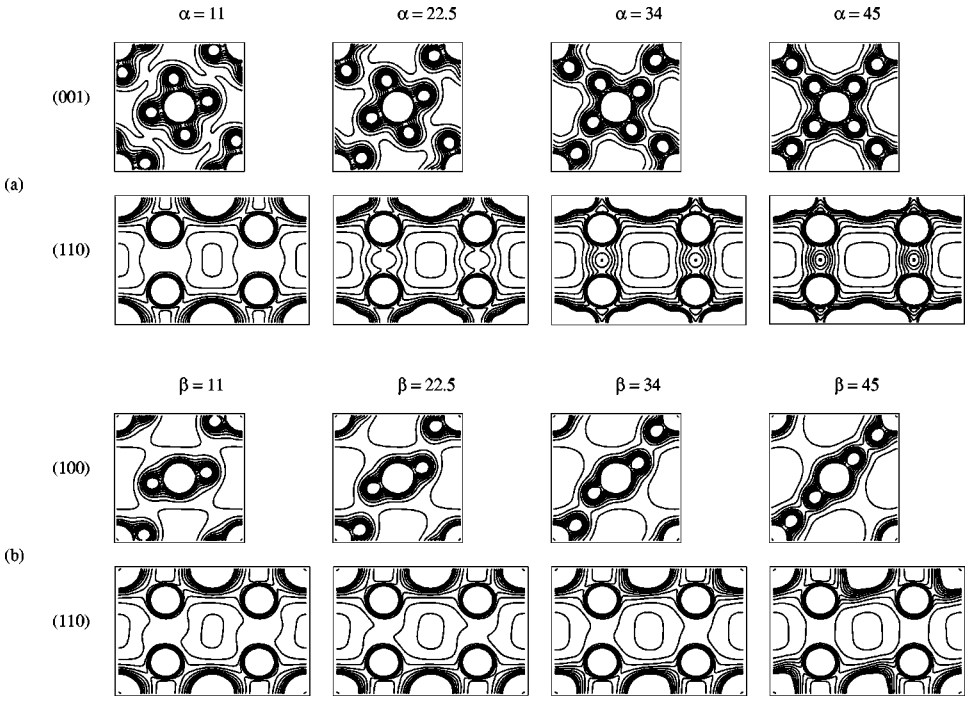

FIG. 3. Electron density contour map of the compound for two sections parallel to different planes of the unit cell for the in-plane α rotation (a) and the out-of-plane β rotation (b). The electron density (electrons $Å^{-3}$) is constant along each of the contour lines.

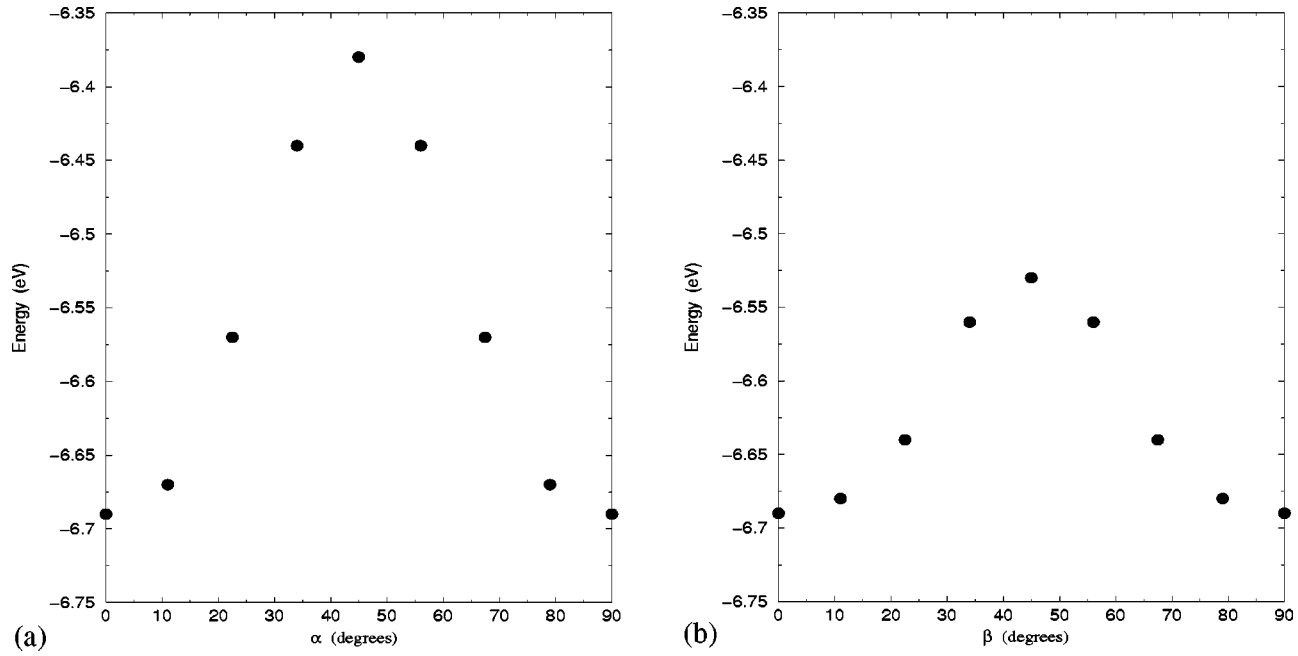

FIG. 4. Calculated activation energy for the in-plane α rotation (a) and the out-of-plane β rotation (b) of the NiH_4 complex. E_c is the energy of formation of the cubic Mg_2NiH_4 with respect to the total free atom energy.

intercomplex interactions increase, which induces a small charge accumulation between them. In particular for the in-plane α rotation, the charge density plots show an increase of charge between the magnesium atoms, which is the projection on the (110) plane of the charge accumulation between the complexes. These results agree with the idea of the existence of a NiH_4 complex in the hydride.[4]

As we mentioned in the previous section, using Eq. (2) we estimate the hydrogen jump frequency by calculation of the attempt jump frequency and the energy barrier. The attempt jump frequency was estimated from a quadratic fit around zero of the energy curve as a function of the rotation angle. The calculated and experimental[9,12,13] values for the attempt jump frequency ν_0 and for the activation energy ΔE are summarized in Table I. Figure 4 shows the total-energy curve as a function of the rotation angle for both diffusion paths.

There is reasonable agreement between the experimental values[9,12,13] and the theoretical results, considering the uncertainty of the measurements and the approximate model used for the calculation.

In Fig. 4 it can be seen that the ΔE for out-of-plane β rotation is about a half of the ΔE for the in-plane α case. It could be associated with the fact that the number of movable hydrogen atoms in the out-of-plane β rotation is half of the number in the in-plane α case. If the hydrogen motion were independent of the neighbor motion in the NiH_4 complex, an activation energy per movable hydrogen atom could be defined approximately equal for both rotations. However, we think that the hydrogen motion is correlated to its neighbors in such a way that the NiH_4 unit moves as a molecule. Thus, ΔE represents the energy to move simultaneously four or two hydrogen atoms as a molecule along the in-plane and out-of-plane rotations, respectively. As a consequence, the out-of-plane jump will be more frequent.

IV. EFFECTS OF THE MOTION ON THE NMR LINE WIDTH PATTERNS

A. Elements of NMR theory

For Mg_2NiH_4, only hydrogen contributes to the relaxation time because magnesium and nickel dipolar interactions are negligible due to their relatively small gyromagnetic ratio. This process is called the spin-lattice relaxation. The resonance absorption line as a function of frequency is not a δ function because the spin-lattice relaxation limits the lifetime of the states and produces a line broadening of the order of $1/T_1$, where T_1 is the spin-lattice relaxation time.

However, there is another process which modifies the relative energy of the energy levels and contributes to the broadening of the resonance line. This is the dipolar interaction between the magnetic moments of the protons in the system, which is called the spin-spin interaction and is characterized by a spin-spin relaxation time T_2. The resonance line broadening is due to the distribution of the local magnetic field produced by the dipolar interaction and is of the order of $1/T_2$.[23]

As a consequence, the resonance line form is described by a shape function $f(\nu)$, which shows the variation of the energy absorption with the frequency around the resonance frequency ν_0. The second moment of the line is used to obtain information about the distribution of protons in the system and its measurement as a function of temperature gives information about atomic diffusion.[24] The second moment is a measure of the mean-squared width of the broadened resonance line $f(\nu)$,

$$\langle \Delta \nu^2 \rangle = \frac{\int_0^\infty (\nu - \nu_0)^2 f(\nu) d\nu}{\int_0^\infty f(\nu) d\nu}. \quad (3)$$

At low temperature, the atoms are in fixed positions (rigid lattice), the local magnetic field is effective to change the Larmor precession of each nucleus, and there is a broadening of the absorption line.[25,26] Van Vleck[25] showed that the mean square of this local field depends on the internuclear distance and on the relative orientation of the internuclear vector with respect to the applied magnetic field, i.e.,

$$\langle \Delta \nu^2 \rangle_{R.L.} = \frac{3}{20\pi^2} \gamma^4 \hbar^2 I(I+1) \sum_j \left(\frac{1}{r_{ij}} \right)^6. \quad (4)$$

When increasing the temperature, the motion of atoms modulates the dipolar interaction and each atom sees the time average of the local magnetic field.[27,28] Bloembergen *et al.*[27] established that only the Fourier components with frequency near zero contribute to the linewidth if the local field is fluctuating, Bloembergen-Purcell-Pound (BPP) theory. This theory considers the motion of the atoms by expanding the factors of the dipolar Hamiltonian that contain the position coordinates in a Fourier series. They redefine the mean square of the dipolar line width as

$$\langle \Delta \nu^2 \rangle = \frac{3}{16\pi^2} \gamma^4 \hbar^2 I(I+1) \int_{-\nu_1}^{\nu_1} J_0(\nu) d\nu. \quad (5)$$

The integral limits are of the order of the linewidth, $\nu_1 = \xi \delta\nu$, where $\delta\nu = \sqrt{\langle \Delta \nu^2 \rangle}$ and $J_0(\nu)$ is the spectral density of a function of the relative coordinates; see the Appendix.

At low temperatures, when all correlation times τ_{cj} are extremely long, Eq. (5) reduces to Eq. (4) for a rigid lattice.

The comparison between the experimental data and our calculation involves the solution of the implicit equation, Eq. (5), for $\delta\nu$. In order to solve Eq. (5), we write the F_{0j} as functions of the angles used to calculate the jump frequency and use for the correlation times the inverse of the calculated jump frequencies. Details of this calculation are given in the Appendix.

B. Calculation of the linewidth

As we mentioned in the previous section, we calculate the second moment of the resonance line because its square root is a measure of the resonance linewidth. Thus, we can compare our results for the activation energy (Sec. III D) with the value obtained experimentally by Hayashi *et al.*[12,13] from measurements of the resonance line (Sec. II). The details of the implicit solution of Eq. (5) are given in the Appendix.

We calculate the second moment for the rigid lattice, taking into account intra- and intercomplex interactions and the narrowing of the line due to the motion within the NiH_4 complex. The obtained solution is the square root of the second moment of the resonance line, $\delta\nu$.

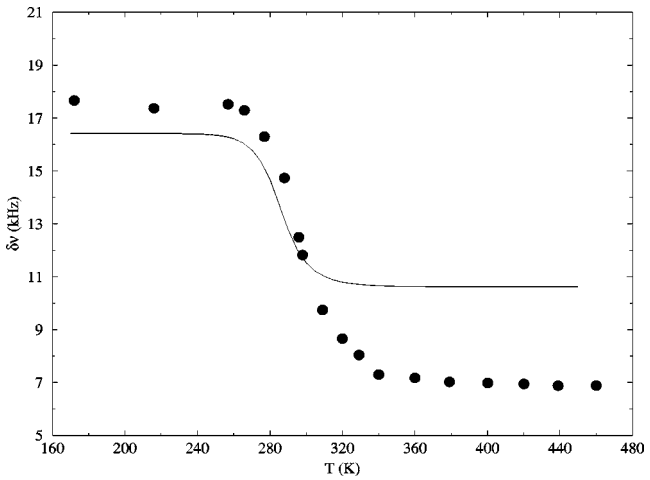

FIG. 5. The solid line corresponds to the calculated linewidth as a function of temperature. The solid marks are the experimental values obtained by Hayashi *et al.* (Ref. 12).

If the shape of the resonance line would be a pure Gaussian distribution, the full width at half intensity is given by $\Delta\nu_{1/2} = 2.35\,\delta\nu$ but this was not the experimental relation. In the experiments, the authors measured the full width at half intensity $\Delta\nu_{1/2}$ and, using Eq. (3), calculated the second moment before and after the narrowing. The shape of the experimental resonance line was very similar to a Gaussian distribution. The constant of proportionality between the experimental full width at half intensity and the square root of the estimated second moment was 2.85 and 2.64 before and after the narrowing, respectively. Hence, to obtain the full width at half intensity, we use a coefficient that is the average of the experimental values, $\Delta\nu_{1/2} = 2.75\,\delta\nu$. Figure 5 shows the calculated full width at half intensity as a function of temperature. In this figure, we show the experimental curve of Hayashi *et al.*[12]

The system for the calculation of the second moment of the rigid lattice consists of 4 protons within a NiH_4 complex plus 48 protons located in the nearest 12 complexes and 24 protons located at the second-neighbor complexes.

We calculate the narrowing that is produced by the motion of protons located in the same NiH_4 complex. Thus, the system consists of four protons. The rotations of the complex average out the local fields produced by intracomplex interactions.

As can be seen in Fig. 5, there is a very good agreement in the temperature range of the narrowing. Thus, as we only consider the motion within the NiH_4 complex, the narrowing can be attributed to the averaging out of the intracomplex interactions, as was suggested by Hayashi *et al.*[12] The theoretical temperature range is between 260 and 350 K, while the experimental range is from 270 to 340 K.

The intracomplex contribution to the second moment is 125.45 $(\mathrm{kHz})^2$ while the inter-complex contribution is 124.93 $(\mathrm{kHz})^2$. These quantities can be calculated using the Van Vleck formula[25] or obtained from the Eq. (A13) if the correlation time τ_c is very long. The sum of these contributions, 250.38 $(\mathrm{kHz})^2$, must be compared with the experimental value, 308.20 $(\mathrm{kHz})^2$. The observed discrepancy at

low temperature in the rigid lattice linewidth can be explained by the presence of paramagnetic impurities, inhomogeneities, or defects in the experimental sample that can produce additional broadening of the resonance line.

The origin of the overestimation of the width of the resonance line at temperatures above 350 K is mainly due to the absence in the calculation of the relaxation of intercomplex interaction produced by the relative motion between complexes. The intercomplex contribution resulting from the interactions between protons belonging to different complexes is affected by the motion of the complexes in a more complicated way, and we do not have first-principles calculations to obtain the correlation time for this kind of motion.

The contribution to the linewidth of the broadening produced by spin-lattice relaxation is neglected. This broadening was estimated using the formula given in Abragam's book[23] and the obtained value is of the order of 10^{-6} kHz. The intercomplex contribution will be lower because the interprotonic distances are greater.

V. CONCLUSIONS

We have studied the localized motion of hydrogen atoms in Mg_2NiH_4 and calculated the jump frequencies for in-plane and out-of-plane rotations of the NiH_4 unit. These jump frequencies are $4\times10^{13}e^{-1.29eV/kT}$ s^{-1} and $3\times10^{13}e^{-0.67eV/kT}$ s^{-1}, respectively.

We have looked for the nickel-hydrogen distance that minimizes the total energy of the rotated planar hydrogen configuration at different rotation angles. In the in-plane α rotation, the nickel-hydrogen distance is about 1.520 Å but tends to decrease with the increment of the rotation angle. For out-of-plane β rotation, the nickel-hydrogen distance along the rotation axis is constant and equal to 1.548 Å, while the nickel-hydrogen distance for hydrogen atoms out of the axis has a similar behavior to the in-plane α rotation. The magnesium-hydrogen distance decreases because the hydrogen position is closer to the magnesium position with the progress of the rotation, but at the same time, the nickel-hydrogen distance decreases. This indicates that the nickel-hydrogen interaction is stronger than the magnesium-hydrogen interaction.

These results support the existence of a NiH_4 complex discussed in our previous work[4] with a characteristic value of the nickel-hydrogen distance of 1.5 Å, in agreement with the experimental value.

Using the results obtained for the jump frequencies, we have calculated the NMR line-width. The obtained results are in good agreement with experimental data. In particular, we remark on the excellent agreement in the result for the temperature range for the narrowing. In view of this result, the narrowing experimentally observed between 270 and 340 K can be understood by considering the relaxation of the interaction among hydrogen atoms within the same complex.

The excellent result for the linewidth calculation, obtained by using the jump frequency determined by total-energy minimization, indicates that the microscopic models for the hydrogen motion proposed here are adequate to describe the real motion and support the idea that the NiH_4 complex is moving as a molecule.

ACKNOWLEDGMENTS

The authors thank Dr. J. Pellegrina for a careful reading of the manuscript and valuable suggestions. This work has been partially supported by the Agencia Nacional de Promoción Científica y Tecnológica (Argentina), BID/OC 1201-PICT 6328. J.O.S. is supported by CONICET (Argentina). G.N.G. is supported by FOMEC (Fondo para el Mejoramiento de la Calidad Universitaria, Argentina).

APPENDIX: CALCULATION OF THE LINEWIDTH

As we mentioned in Sec. IV B, we will resolve Eq. (5) as a function of temperature for a system of four hydrogen atoms that form the NiH_4 unit. The solution of Eq. (5) involves the calculation of $J_0(\nu)$ defined by[27]

$$J_0(\nu)=\sum_{j=1}^{3}\int_{-\infty}^{\infty}K_{0j}(\tau)e^{2\pi i\nu\tau}d\tau, \tag{A1}$$

with

$$K_{0j}(\tau)=\langle F_{0j}^{*}(t+\tau)F_{0j}(t)\rangle=\langle F_{0j}^{*}(t)F_{0j}(t)\rangle e^{-\tau/\tau_c} \tag{A2}$$

and

$$F_{0j}(t)=(1-3\cos\theta_{ij})r_{ij}^{-3}. \tag{A3}$$

The sum runs over pairs of magnetic nuclei; F_{0j} represents the dipolar interaction dependence with the relative coordinates of each pair, and K_{0j} is the correlation function of F_{0j}; τ_c is the correlation time.

The objective is to write the dipolar interaction as a function of the rotation angles considered to calculate the attempt jump frequencies and the activation energies (Sec. III D).

The starting point is to write the cosine of the angle between the internuclear vector with the steady magnetic field as a function of trigonometric functions of the working angles. These expressions are

$$\cos\theta_1=\frac{1}{\sqrt{2}}\sin\beta(\cos\alpha-\sin\alpha),$$

$$\cos\theta_2=-\sin\beta\sin\alpha,$$

$$\cos\theta_3=-\frac{1}{\sqrt{2}}\sin\beta(\cos\alpha+\sin\alpha). \tag{A4}$$

Now, we have to write Eq. (A3) for each pair as a function of α and β:

$$F_{01}=\frac{1}{a^3}-\frac{3}{2a^3}\sin^2\beta+\frac{3}{2a^3}\sin 2\alpha,$$

$$F_{02}=\frac{1}{b^3}-\frac{3}{b^3}\sin^2\beta\sin^2\alpha,$$

$$F_{03}=\frac{1}{a^3}-\frac{3}{2a^3}\sin^2\beta-\frac{3}{2a^3}\sin 2\alpha. \tag{A5}$$

To calculate the correlation function $K_{0j}(\tau)$, each one of the $F_{0j}(t)$ may be written as a sum of terms composed by the multiplication of functions $A(\alpha)$, $B(\beta)$, and $C(r)$, i.e.,

$$K_{0j}(\tau)=\sum_{l,m=1}^{3}\langle A_l^*(t')B_l^*(t')C_l^*(t')A_m(t)B_m(t)C_m(r)\rangle, \tag{A6}$$

where

$$t'=t+\tau.$$

As a consequence of the independence of the two motions, each term of the average is written as a product of average of terms in $A(\alpha)$, in $B(\beta)$, and in $C(r)$:

$$K_{0j}(\tau)=\sum_{l,m=1}^{3}\langle A_l^*(t')A_m(t)\rangle\langle B_l^*(t')B_m(t)\rangle \times\langle C_l^*(t')C_m(t)\rangle. \tag{A7}$$

Using the same assumption as in the BPP theory, the time average of each factor in the previous formula is calculated as

$$\langle A_l^*(t+\tau)A_m(t)\rangle=\langle A_l^*(t)A_m(t)\rangle e^{-t/\tau_{out}},$$

$$\langle B_l^*(t+\tau)B_m(t)\rangle=\langle B_l^*(t)B_m(t)\rangle e^{-t/\tau_{in}},$$

$$\langle C_l^*(t+\tau)C_m(t)\rangle=\langle C_l^*(t)C_m(t)\rangle e^{-t/\tau_m}, \tag{A8}$$

where $\tau_{out}=1/\nu_{out}$ and $\tau_{in}=1/\nu_{in}$ are the inverses of the jump frequencies calculated here using first-principle calculations, and $1/\tau_m=1/\tau_{out}+1/\tau_{in}$. After some algebra, the correlation functions are obtained:

$$K_{01}=\frac{4}{5a^6}e^{-t/\tau_c},$$

$$K_{02}=\frac{4}{5b^6}e^{-t/\tau_c},$$

$$K_{03}=\frac{4}{5a^6}e^{-t/\tau_c}, \tag{A9}$$

where $1/\tau_c=2/\tau_m$.

Now, we have to calculate the Fourier transform of these expressions to have $J_0(\nu)$ [Eq. (A1)]:

$$J_0(\nu)=\frac{8(a^6+2b^6)}{5a^6b^6}\frac{\tau_c}{1+4\pi^2\nu^2\tau_c^2}. \tag{A10}$$

To obtain the dipolar contribution to the linewidth it is necessary to replace the $J_0(\nu)$ expression in the implicit equation for $(\delta\nu)^2$ [Eq. (5)]:

$$(\delta\nu)^2=C\frac{a^6+2b^6}{a^6b^6}\tan^{-1}(2\pi\xi\tau_c\delta\nu), \tag{A11}$$

with

$$C=\frac{6}{5\pi}\gamma^2\hbar^2I(I+1). \tag{A12}$$

This equation gives us the linewidth in units of the magnetic field, and the conversion to frequency units is done multiplying by $(\gamma/2\pi)^2$. Replacing the values of γ, $\hbar$, and $I=1/2$, and using $a=2.189\,10^{-8}$ cm, $b=3.096\,10^{-8}$ cm, and $\xi=1$, the dipolar linewidth must verify

$$(\delta\nu)^2=79.9094\tan^{-1}(2\pi\tau_c\delta\nu)+124.928. \tag{A13}$$

The additive constant represents the contribution to the second moment of the intercomplex interactions. The units of the linewidth are kHz.

The full width at half intensity is obtained using $\Delta\nu_{1/2}=2.75\,\delta\nu$.

*Author to whom correspondence should be addressed. Electronic address: garciag@cab.cnea.gov.ar

[1] G. Sandrock, S. Suda, and L. Schlapbach, *Topics in Applied Physics, Hydrogen in Intermetallic Compounds II* (Springer, Berlin, 1992), Vol. 67, p. 210; P. Dantzer, *Topics in Applied Physics, Hydrogen in Metals III* (Springer, Berlin, 1997), Vol. 73, p. 279.

[2] J.J. Reilly and R.H. Wiswall, Jr., Inorg. Chem. **7**, 2254 (1968).

[3] P. Villars, A. Prince, and H. Okamoto, *Handbook of Ternary Phase Diagrams* (American Society for Metals, Metals Park, OH, 1995), Vol. 9, p. 11 659.

[4] G.N. García, J.P. Abriata, and J.O. Sofo, Phys. Rev. B **59**, 11 746 (1999). We note an error occurred in Table I of this reference; the energy values are given in eV/H atom instead of eV/formula. This mistake does not affect the results and conclusions obtained.

[5] P. Zolliker, K. Yvon, J.D. Jorgensen, and F.J. Rotella, Inorg. Chem. **25**, 3590 (1986).

[6] Z. Gavra, M.H. Mintz, G. Kimmel, and Z. Hadari, Inorg. Chem. **18**, 3595 (1979).

[7] J. Genossar and P.S. Rudman, J. Phys. Chem. Solids **42**, 611 (1981).

[8] K. Yvon, J. Schefer, and F. Stucki, Inorg. Chem. **20**, 2776 (1981).

[9] D. Noréus and L.G. Olsson, J. Chem. Phys. **78**, 2419 (1983).

[10] B. Darriet, J.L. Soubeyroux, M. Pezat, and D. Fruchart, J. Less-Common Met. **103**, 153 (1984).

[11] S. Goren, C. Korn, M. Mintz, Z. Gavra, and Z. Hadari, J. Chem. Phys. **73**, 4758 (1980).

[12] S. Hayashi, K. Hayamizu, and O. Yamamoto, J. Chem. Phys. **79**, 2308 (1983).

[13] S. Hayashi, K. Hayamizu, and O. Yamamoto, J. Chem. Phys. **79**, 5572 (1983).

[14] M. Gupta, J. Less-Common Met. **101**, 35 (1984); M. Gupta, E. Belin, and L. Schlapbach, *ibid.* **103**, 389 (1984).

[15] Y. Fukai, *The Metal-Hydrogen System: Basic Bulk Properties*

(Springer, Berlin, 1992), Vol. 21.
[16] P. Blaha, K. Schwarz, and J. Luitz, computer code WIEN97, Vienna University of Technology, 1997. [Improved and updated Unix version of the original copyrighted WIEN code, published by P. Blaha, K. Schwarz, P. Soratin, and S.B. Trickey, in Comput. Phys. Commun. **59**, 399 (1990)].
[17] D. Singh, *Plane Waves, Pseudopotentials, and the LAPW Method* (Kluwer Academic, New York, 1994).
[18] J.P. Perdew and Y. Wang, Phys. Rev. B **45**, 13 244 (1992).
[19] D. Singh, Phys. Rev. B **43**, 6388 (1991).
[20] *International Tables for Crystallography*, edited by Theo Hahn (Kluwer Academic, Dordrecht, 1992).
[21] K. W. Kehr, *Topics in Applied Physics, Hydrogen in Metals 1: Basic Properties* (Springer, Berlin, 1978), Vol. 28, p. 197.
[22] H. Eyring, J. Chem. Phys. **3**, 107 (1932); C. Wert and C. Zener, Phys. Rev. **76**, 1169 (1949); G.H. Vineyard, J. Phys. Chem. Solids **3**, 121 (1957); C.P. Flynn, *Point Defects and Diffusion* (Clarendon Press, Oxford, 1972), p. 319.
[23] A. Abragam, *The Principles of Nuclear Magnetism* (Oxford University Press, London, 1961); E. R. Andrew, *Nuclear Magnetic Resonance* (Cambridge University Press, Cambridge, England, 1958).
[24] C. Kittel, *Introduction to Solid State Physics* (Wiley, New York, 1986), p. 470.
[25] J.H. Van Vleck, Phys. Rev. **74**, 1168 (1948).
[26] H.S. Gutowsky, G.B. Kistiakowsky, G.E. Pake, and E.M. Purcell, J. Chem. Phys. **17**, 972 (1949).
[27] N. Bloembergen, E.M. Purcell, and R.V. Pound, Phys. Rev. **73**, 679 (1948).
[28] H.S. Gutowsky and G.E. Pake, J. Chem. Phys. **18**, 162 (1950).